Available online at www.sciencedirect.com
SCIENCE DIRECT
Biochimica et Biophysica Acta 1714 (2005) 11 – 24
BIOCHIMICA ET BIOPHYSICA ACTA
BBA
http://www.elsevier.com/locate/bba

Charge patch attraction and reentrant condensation in DNA–liposome complexes

S. Sennato[a], F. Bordi[a], C. Cametti[a,*], M. Diociaiuti[b], P. Malaspina[c]

[a]Dipartimento di Fisica, Universita' di Roma "La Sapienza", Piazzale A. Moro 5, I-00185-Rome (Italy) and INFM-CRS SOFT, Unita' di Roma1
[b]Dipartimento di Tecnologie e Salute, Istituto Superiore di Sanita', Rome, Italy
[c]Dipartimento di Biologia, Universita' di Roma "Tor Vergata", Via della Ricerca, Scientifica I-00133 Rome, Italy

Received 28 October 2004; received in revised form 26 April 2005; accepted 7 June 2005
Available online 28 June 2005

Abstract

We investigated the formation of complexes between cationic liposomes built up by DOTAP and three linear anionic polyions, with different charge density and flexibility, such as a single-stranded ssDNA, a double-stranded dsDNA and the polyacrylate sodium salt [NaPAA] of three different molecular weights. Our aim is to gain further insight into the formation mechanism of polyion–liposome aggregates of different sizes (lipoplexes), by comparing the behavior of DNA with a model polyelectrolyte, such as NaPAA, with approximately the same charge density but with a higher flexibility. We employed dynamic light scattering (DLS) and transmission electron microscopy (TEM) measurements, in order to explore both the hydrodynamic and structural properties of the aggregates resulting from polyion–liposome interaction and to present a comprehensive picture of the complexation process. The phenomenology can be summarized in a charge ratio-dependent scenario, where the main feature is the formation of large *equilibrium* clusters due to the aggregation of intact polyion-coated vesicles. At increasing polyion–liposome ratio, the size of the clusters continuously increases, reaching a maximum at a well-defined value of this ratio, and then decreases ("reentrant" condensation). The aggregation mechanism and the role of the polyion charge density in the complex formation are discussed in the light of the recent theories on the correlated adsorption of polyelectrolytes at charged interfaces. Within this framework, the phenomena of charge inversion and the reentrant condensation, peaked at the isoelectric point, finds a simple explanation.

Keywords: DNA; Lipoplexes; Charge inversion; Reentrant condensation

1. Introduction

A variety of biomedical applications employs cationic lipid–DNA complexes (lipoplexes) as preferential DNA delivery vehicles in gene therapy [1–3]. It is well known that the complexation of negatively charged DNA with cationic liposomes helps the delivery of DNA into the cell nucleus, by facilitating binding to the negatively charged cell surface and by aiding the DNA penetration into the cytosol [4].

The problem of the interaction of DNA with cationic liposomes has been approached from different points of view. Numerous studies, aimed to improve the understanding of the basic mechanism of lipoplex transfection, suggest that the efficiency of the whole process depends critically on the physical and chemical properties of lipoplexes [5]. Many investigations focused on the gene transfer efficiency of various cationic liposome formulations [6–8], showing how the composition and the colloidal properties of the complexes had major effects [9–11]. Other investigations deal with the supra-molecular structure of liposome–DNA complexes, in order to clarify possible structure–function correlations [12–16]. Although significant efforts have been carried out in the study of these structures, the physical processes occurring during lipoplex self-assembly remain largely unclear.

From a theoretical point of view, the interaction of DNA with cationic liposomes is related to the electrostatic

* Corresponding author. Fax: +39 06 4463158.
E-mail address: cesare.cametti@roma1.infn.it (C. Cametti).

0005-2736/$ - see front matter © 2005 Elsevier B.V. All rights reserved.
doi:10.1016/j.bbamem.2005.06.004

adsorption of charged macromolecules onto an oppositely charged surface. This problem has been recently addressed by several authors (see, for example, [17–22]). The underlying physics is interesting and shows unexpected features such as the counterintuitive phenomenon of 'charge inversion' [17,23,24] and the formation of large aggregates close to the isoelectric point ('reentrant condensation'). These effects are caused by the strong lateral correlation among the polyions adsorbed onto the charged surface [17,18,21]. Adsorbed polyions are not positioned at random and correlations occur because they reconfigure themselves in a short-range order [25,26] to gain some energy. The complex surface appears decorated by a more or less ordered 'patchwork-like' pattern, with excess negative charge domains (polyelectrolyte domains) and excess positive charge (polyelectrolyte free) domains. From such a non-homogeneous surface charge distribution, a short range, "dipolar", attractive potential arises ("charge patch" attraction) [27,28]. Hence, close enough to the isoelectric point, the relatively small electrostatic repulsion balances this 'charge patch' attraction and lipoplexes aggregate, forming large equilibrium clusters.

The phenomenology of DNA–cationic liposome interaction appears rather complex, depending on many parameters such as the charge density on the particle surface and on the polyion chain, the flexibility of the polyion backbone and the physical–chemical properties of the medium. As a consequence, a complete characterization of the resulting complex structure is still lacking.

Only recently, the role of the overall charge density of lipoplexes has been put into evidence [11], while the effects of counterions on the complexes formation are still not completely clear. The importance of the counterion release was pointed out by Rädler et al. [14], who identified this phenomenon as the driving force for the DNA–liposome aggregation. In solution, a highly charged linear polyion, such as DNA, is surrounded by a certain fraction of its counterions, which result confined along the chain ("condensed" counterions) [29]. According to Rädler et al. [14] and Bruinsma [30], when a DNA chain fuses with a cationic liposome, counterions of both polyelectrolytes and the phospholipids are released to the bulk. This mechanism is supposed to play a key role in the organization of lipoplexes [30–32].

From the above scenario, it appears that a better understanding of the counterions role in the complexation process is required. Classical electrical measurements (surface pH, zeta potential and electrophoretic mobility) proved to be important in supporting evidence of the electrostatic interactions in polyelectrolyte/liposome complexation, but not sufficient to completely clarify the basic mechanisms for lipoplex formation.

In this study, in order to gain further insight into these mechanisms, we have compared the behavior of different linear polyions, differing for charge density and flexibility, in their interaction with highly charged cationic liposomes, supporting of evidence the role of polyion correlated adsorption and of condensed counterion in the lipoplex formation and equilibrium character of these aggregates.

In the present study, we compare the behavior of double stranded DNA [ds-DNA] with two different polyions: a single stranded DNA [ssDNA], characterized by a much lower charge density, and polyacrylate sodium salt [NaPAA], with approximately the same charge density but a much higher flexibility. As a model system for cationic liposomes, unilamellar vesicles built up by cationic lipid dioleoyltrimthylammoniumpropane [DOTAP] were employed.

In order to present a comprehensive scenario of the complexation process, we employed two different experimental techniques, dynamic light scattering (DLS) and transmission electron microscopy (TEM) measurements. This strategy is intended to provide further insight in the complexation process with the aim to reconcile the pictures emerging from different spectroscopic and structural techniques [14,33–35], in the light of the more recent theories on macroion-charged surface interactions.

We investigated the size, size distribution and the morphology of lipoplexes in a wide polyion concentration range. For all the polyions investigated, with the increase of the charge ratio, polyion-coated liposomes aggregate in *equilibrium* clusters whose size increases continuously with polyion content and where the vesicles maintain their individuality. Close to the 'isoelectric' point, cluster size reaches its maximum value, while further addition of polymer results in a continuous decrease of cluster size ("reentrant" condensation). While this qualitative behavior is observed for all the three polyions employed, both the maximum size reached by the aggregates and the charge ratio value where this maximum is attained apparently depend on the degree of polymerization of the polyion and on its charge density. Moreover, the presence of a simple electrolyte (NaCl) in the suspension has a dramatic effect in the aggregation process.

We present a comprehensive picture to explain the overall observed behavior, on the basis of the more recent theories on polyion *correlated* adsorption and *charge patch* attraction between DNA–liposome complexes.

2. Experimental

2.1. Materials

Single-stranded calf thymus DNA (ssDNA) was purchased from Sigma Chem. Co. In these samples, polydispersity ranges between 590 and 830 base pairs. Double-stranded herring sperm DNA (dsDNA) was purchased from Boehringer Mannheim, GmbH. The sample is rather polydisperse and the length of the fragments ranges from 100 to 600 base pairs. Polyelectrolyte samples were polyacrylate sodium salt $[\text{-}CH_2CH(CO_2N_a)\text{-}]_n$, [NaPAA], with nominal molecular weight 5.1, 60 and 225 kDa, purchased from Polysciences Inc. (Warrington, PA) as 25%

aqueous solution. The lipid dioleoyltrimethylammonium-propane [DOTAP] was purchased from Avanti Polar Lipids (Alabaster, AL) and used without further purification. Gold-labeled streptavidin was purchased from Sigma Chem. Co. (10 nm gold particles at a concentration of 1.6×10^{13} particle/ml).

2.2. Preparation of cationic lipid–polyion complexes

Liposomes were prepared by dissolution of appropriate amount of DOTAP (17 mg) in 10 ml methanol–chloroform solution (1:1 vol/vol). An overnight vacuum evaporation of the solvent results in a dried lipid film, which was then re-hydrated with Milli-Q quality water (electrical conductivity less than 1×10^{-6} mho/cm, pH ≈ 6.3). Re-hydration was carried out for 1 h at a temperature of 25 °C, well above the main phase transition temperature of this lipid (T_f=0 °C). In order to form unilamellar vesicles, the lipid solution was sonicated at a temperature of 25 °C for 1 h at a pulsed power mode, until the solution appeared optically transparent in white light. The solution was then filtered by means of Millipore 0.4 μm polycarbonate filter. The final liposome concentration was 1.5×10^{13} particle/ml and the solution was stored at 4 °C. The mean hydrodynamic radius of the DOTAP liposomes was about 40 nm and the size distribution was log-normal with a polydispersity of the order of 0.2–0.25.

As we have already observed in a preliminary investigation [36], these liposomes, in the absence of added salt or polyelectrolytes, are very stable in time, from several days to a few weeks. This is probably due to electrostatic interactions which, combining the effect of the charge density to the curvature moduli [37,38], tend to stabilize the bilayer curvature. The polyion–liposome complex formation was promoted by adding 250 μl of polyion solution (prepared at an appropriate concentration) to an equal volume of liposome suspension in a single mixing step and gently shaking by hand, with a final liposome concentration of 7.5×10^{12} particle/ml. This procedure has been followed for all the experiments. As already observed by Zuidam et al. [9], neither the complex formation nor the resulting aggregate size was essentially influenced nor by the order of addition of polyion and liposome, nor by the use of a vortex for mechanical mixing. In the case of single stranded DNA, in order to avoid strand annealing, DNA samples were stocked at −20 °C and thawed immediately before mixing with liposomes. Since single strand DNA re-associates, at room temperature, at a very low rate (a few percent in several hours, [39]), and from DLS measurements, the process is apparently completed in less than a minute, all the adsorbed DNA can be considered in single strand form. Dynamic light scattering measurements were performed within 10 min after mixing liposome and polyion solutions. All experiments were carried out at a controlled temperature of 25.0 ± 0.2 °C and were repeated several times to check reproducibility.

2.3. Preparation of gold-labeled liposome aggregates

In order to better characterize the DNA-induced liposome aggregates, we investigated liposome complexes using biotinylated DNA. To create liposome aggregates, 0.015 ml of liposome suspension prepared at a concentration C=1.6 mg/ml and 0.015 ml of biotinylated DNA at a concentration C=0.36 mg/ml were mixed together. This procedure created vesicle aggregates which have several biotin ligands protunding from the exterior surface. An aqueous dispersion of gold-labeled streptavidin molecules, which have a high affinity [40] with biotin, was then added to the liposome aggregates, giving rise to complexes formed in a cross-linking network where binding events at the aggregate surface lead to a detectable concentration of gold particles.

Biotin-labeled DNA fragments were obtained by polymerase chain reaction (PCR) [41] in the presence of biotin-14-dCTP (Invitrogen) and using as template a plasmid clone containing human genomic DNA (GenBank Accession No. Y11192). Plasmid DNA (300 mg) was amplified in 50 ml reaction containing 1× reaction buffer, 1.5 mM $MgCl_2$, 1 U TaqI polymerase (Promega), 100 μM dNTP-dCTP, 65 μM dCTP, 40 μM biotin-14-dCTP (Invitrogen), 0.2 μM S2 (5′-TCCAGTGCCATGATCAC-3′) sense and L3b (5′-AATAATGGATG-GCATGTACC-3′) antisense primers [42]. Ten separate PCR reactions were performed under the following conditions: initial denaturation step at 94 °C for 5 min was followed by 35 cycles of denaturation (94 °C for 1 min), primer annealing (52 °C for 1 min) and extension (72 °C for 1 min). The 1060-bp amplified product was analyzed on 1.5% agarose gel. A total amount of PCR product of about 25 μg was obtained. Following the labeling reactions, unincorporated nucleotides were separated from biotinylated DNA fragments by sodium acetate and ethanol precipitation [41]. After two washes with 70% ethanol, DNA was resuspended in 70 μl of sterile and deionized water. Biotin-labeled DNA can hence be easily and specifically localized in TEM images by using streptavidin conjugated to colloidal gold.

2.4. Dynamic light scattering measurements

Dynamic light scattering (DLS) measurements were employed to characterize the size and size distribution of liposomes and of the liposome–polyion complexes. The apparatus used was a spectrometer equipped with a Brookhaven BI9000AT logarithmic correlator and a 10-mW HeNe laser source of wavelength 632.8 nm. Light scattered by the sample, placed in a thermostatted bath maintained at a temperature of 25.0 ± 0.2 °C was detected at an angle of 90 °. We measured the normalized time autocorrelation function of the intensity of the scattered light $g^{(2)}(\tau)$ that can be expressed in terms of the electric field autocorrelation function $g^{(1)}(\tau)$ through the Siegert relationship.

For a dilute suspension of monodisperse particles, the dynamic structure factor $f(\tau)$ decays exponentially with a

decay rate $\Gamma = q^2 D$, where q is the magnitude of the scattering wavevector and D the translational diffusion coefficient which is related to the hydrodynamic radius R_H through the Stokes–Einstein relationship

$$R_H = \frac{K_B T}{6\pi\eta D} \quad (1)$$

where $K_B T$ is the thermal energy and η the viscosity of the medium [43]. For a polydisperse system, $f(\tau)$ can be expressed as

$$f(\tau) = \int_0^\infty G(\Gamma)\exp(-\Gamma\tau)d\Gamma \quad (2)$$

where the distribution of decay rates, corresponding to particles with a different size, is given by the function $G(\Gamma)$. The determination of this distribution requires the inversion of Eq. (2). Methods based on "a priori" hypotheses on the shape of multi-modal distributions [44,45] are of limited applicability. Without any hypothesis on the distribution shape, Eq. (2) can be solved for $G(\Gamma)$ by numerical methods. Unfortunately, it has been proved that this problem, from the mathematical point of view, is an "ill-posed problem", i.e., many (and often quite different) distributions $G(\Gamma)$ exist whose transforms fit the measured data within experimental error [44,46]. Different procedures have been proposed to overcome this difficulty. Within the 'regularization' techniques, the best size distribution is selected by using constrained minimization based on a "simplicity" criterion: the simplest solution (usually the one showing the smallest number of peaks) is selected [44,47]. As to be expected, in many practical cases different regularization methods furnish different results. In all these cases, an even more careful analysis of DLS data is needed. As a rule of thumb, this analysis should proceed along two (quite obvious) steps: taking repeated data sets on the same sample and eventually averaging the final distribution; analyzing each data set by means of different algorithms, comparing the characteristics of the distributions obtained from the different methods, possibly rejecting the features that seem to be method-dependent.

In our analysis, after a preliminary cumulant analysis [43], used as a screening method to exclude possible artifacts due to the presence of dust or very large aggregates, we employed for each data set (from three to ten, or more, for each sample) both the standard regularization algorithm CONTIN [48,49] and the 'Non-Negative Least Squares' (NNLS) algorithm of [50].

2.5. TEM measurements

Samples for Transmission Electron Microscopy (TEM) measurements were prepared by deposition of a droplet of the suspension containing the liposome–polyion complexes onto a 300-mesh copper grid for electron microscopy, which was covered by 20 nm thin amorphous carbon film. The excess liquid was withdrawn by touching the grid to filter paper. Before samples were completely dried, 10 μl of 2% aqueous phosphotungstic acid [PTA] solution (pH adjusted to 7.3 using 1 N NaOH) was used as staining solution. In order to eliminate impurity, the solution was filtered by polycarbonate 0.2 μm filters before deposition. In a few cases, grids have been made hydrophilic by using the glow-discharge method [51] in order to ascertain interaction between the grid and the sample and possible consequent artifacts on the sample morphology.

For biotinylated samples, the grid with the deposited sample was floated face down on a 20-μl drop of the solution (phosphate-buffered saline (PBS), pH 7.2, 1% of bovine serum albumin (BSA), 20% glycerol and 15 mM sodium azide) containing the streptavidin-conjugated colloidal gold particles with a diameter of 10 nm for immuno-staining and incubated at room temperature for 45 min. Grids were then washed 2×5 min in 30 μl drops of PBS with 1% BSA and 2×5 min in deionized water. The excess liquid was then withdrawn by touching the grid to filter paper.

The microscope was a ZEISS 902 operating at 80 kV, equipped with an Electron Energy Loss Filter. Moreover, Electron Spectroscopy Imaging (ESI) mode was used in order to enhance image contrast. Image acquisition was performed by a digital CCD camera mod. PROSCAN HSC2 ($1\,k \times 1\,k$ pixels) thermostated by a Peltier cooler. The analysis was carried out by a digital analyzer SIS 3.0 which allows to enhance contrast and sharpness of the acquired images and to perform morphological quantification and statistics. The overall resolution can be estimated in the order of 2 nm.

PTA negative staining demonstrates a simple and effective technique to enhance the contrast in liposome aggregate images [52]. We checked the absence of major artifacts that, in principle, the interaction of the acidic PTA with cationic lipid could introduce, by comparing images where negative staining was employed, with images obtained by using ESI mode, without any chemical staining. In many cases, although the negative staining greatly improves the image quality, the main features of the structures are also recognized in the images obtained by ESI mode.

3. Results

The evolution of the size and size distribution of the polyelectrolyte/cationic liposome complexes were directly monitored by the behavior of their apparent hydrodynamic radius R_H, obtained from DLS. This process was studied in a wide polyion concentration range, from dilute to semi-dilute regime. On each liposome–polyion sample, we performed repeated DLS measurements, single measurement lasting 3 min, for a total acquisition time of 180 min or more. Each sample was *stable* in time, the complexes exhibiting a unimodal log-normal distribution, both when analyzed by CONTIN and by NNLS, whose mean value and

width remain unchanged during the whole acquisition time. In Figs. 1 and 2, we report the mean value of the measured lipoplex radii for the three polyions investigated (ssDNA, dsDNA and NaPAA).

In order to present the results in a unified way, we define a "stoichiometric" charge ratio parameter N^-/N^+ as the ratio between the total number N^- of the negative charges on the polyion and the total number N^+ of the positive charges on DOTAP molecules in the whole suspension

$$\frac{N^-}{N^+} = \frac{C_M}{Mw_M}\frac{Mw_D}{C_D} \quad (3)$$

where C_M and C_D are the (weight) concentrations of the polyion and DOTAP into the sample solution, respectively, and Mw_M and Mw_D are the molecular weight of the repeating unit of the polyion and the molecular weight of DOTAP. In all the experiments, the concentration of DOTAP was fixed to the value of 0.85 mg/ml. With this definition of N^-/N^+ , all the charges on the liposomes are considered, both on the outer and on the inner leaflet of the vesicle; analogously, as far as polyion charges are concerned, a full ionization is conjectured, counterion condensation being not introduced yet.

The evolution of the hydrodynamic radius for the complexes of DOTAP liposomes with double-stranded dsDNA and single-stranded ssDNA, at increasing N^-/N^+ charge ratio is shown in Fig. 1, (panels A and B), respectively. At low polyion content, the hydrodynamic radius of the complexes is about 50 nm, for both the polyions, very close, within the experimental uncertainties, to the one of pure liposomes. With the increase of polyion content, the size of the complexes gradually increases until a maximum is reached, of the order of 250 nm for dsDNA and 150 nm for ssDNA. A further increase in polyion content determines the formation of decreasing size complexes, until the size of the original liposomes is again approximately attained. In summary, a monotonous increase of the charge ratio causes a non-monotonous change in the size of the aggregates, showing a peak at a well defined value of N^-/N^+ ("reentrant" condensation). Similar results have been reported by Lai and van Zanten and by Pires et al. [53–55] for DNA-DOTIM/cholesterol cationic liposomes, and by Rädler et al. [56] for DOPC/DOTAP–DNA complexes. Although both ssDNA and dsDNA show a similar behavior, the width of the concentration range, where the "reentrant" condensation takes place, and the position of the peak are well distinct in the two cases. Maximum is obtained at a charge ratio $N^-/N^+ \sim 0.2$ for ssDNA, and $N^-/N^+ \sim 1$ for dsDNA (Fig. 1).

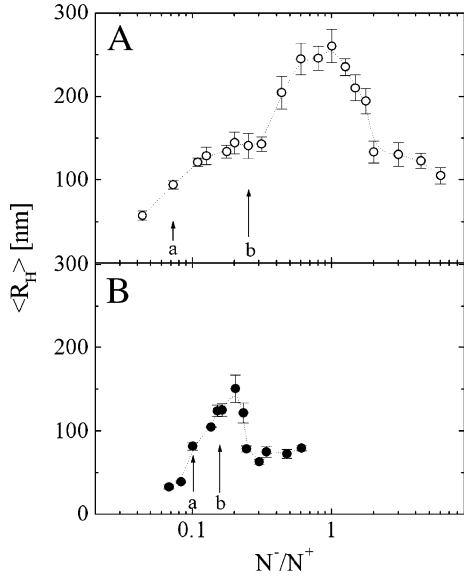

Fig. 1. The average hydrodynamic radius $<R_H>$ of DNA-DOTAP complexes as a function of the DNA/DOTAP N^-/N^+ charge ratio parameter, for the different investigated polyions; panel A: double stranded (ds)DNA; panel B: single stranded (ss)DNA. Letters mark the polyion/lipid charge ratio at which TEM measurements have been carried out (see Figs. 3–6).

Measurements of ssDNA have been performed in a wider charge ratio range than that showed in Fig. 1. Data from $N^-/N^+ > 0.6$ to $N^-/N^+ \approx 4$ are not shown since at these concentrations a non-equilibrium regime takes place. However, the reentrant condensation is apparently concluded at a charge ratio slightly below the value of $N^-/N^+ = 1$. Above this value, a different regime appears and the liposome suspension is almost immediately flocculated by the addition of such a large amount of polyelectrolyte. This is exactly what happens, although at a higher charge ratio, also in the case of dsDNA and NaPAA [36] and also in the presence of high content of NaCl electrolyte solution [35]. At large polyelectrolyte excess, electrostatic interactions are so screened that a flocculation process takes place (DLVO theory [57]). This phenomenology is clearly different from the reentrant condensation we focus on in this paper.

Fig. 2 summarizes the hydrodynamic radius evolution for the complexes formed when NaPAA polyion at different molecular weights is added to the liposome suspension. NaPAA concentration ranges from 0.005 to about 1 mg/ml, so that for all the molecular weights investigated the polyion is in the dilute regime [58]. The phenomenology is similar to that observed for DNA; the maximum in size of complexes is localized at a charge ratio close to $N^-/N^+ = 1$, as for dsDNA. Also in this case, as the polyion concentration is further increased, above $\approx N^-/N^+ > 10$, a different regime takes place (data not shown) and non-equilibrium aggregates larger than $2 \div 3$ μm form.

We employed Transmission Electron Microscopy (TEM) measurements to interpret the morphology of the various NaPAA– and DNA–DOTAP complexes. TEM technique applied to negatively stained liposome structures has been shown to be appropriate to study the formation and the morphology of liposomal aggregates of different sizes [59]. TEM measurements were carried out on various samples of polyion–liposome complexes, already characterized by DLS; according to these results, we chose samples at significant charge ratios.

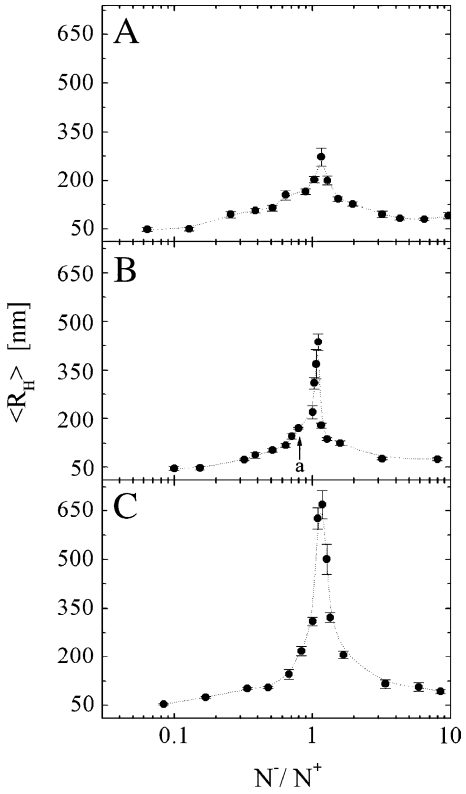

Fig. 2. The average hydrodynamic radius $<R_H>$ of NaPAA-DOTAP structures as a function of NaPAA/DOTAP N^-/N^+ charge ratio, for different molecular weights: (A): M_w=5.1 kDa; (B): M_w=60 kDa; (C): M_w=225 kDa. In panel B, the letter (a) indicates the polyion concentration at which TEM image shown in Fig. 8 has been carried out.

Fig. 3 shows the structures formed when dsDNA is added to the liposome suspension, to a charge ratio of N^-/N^+=0.07 (sample marked by letter a) in Fig. 1, panel A. At this charge ratio, complexation results in the formation of isolated polyion-coated liposomal particles and no larger structures are observed. Negative staining evidences the spheroidal shape of the vesicles and reveals a diffuse pattern surrounding each particle, presumably due to the adsorbed dsDNA. The thickness of this layer can be estimated in the order of 5 nm. This estimate is probably affected by large uncertainties due to the possible effects of interaction between PTA and charged groups at the aggregate surface. However, in samples prepared from the same stock liposome suspension, in the absence of added polyions, no surface pattern is observed (images not shown).

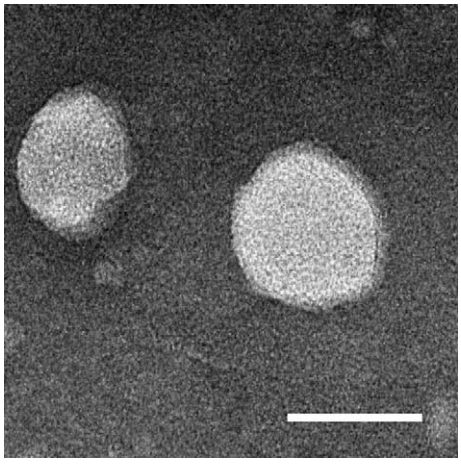

Fig. 3. TEM image (negative staining) of dsDNA–DOTAP complexes at N^-/N^+=0.07, (concentration marked by the letter a) in panel A of Fig. 1). Liposomes appear isolated, with the adsorbed polyions that form a diffuse layer on the surface, well visible at the border of the vesicles. Bar represents 100 nm.

At higher polyion content, well definite changes in the vesicle morphology are observed (Fig. 4; charge ratio N^-/N^+=0.25, sample b) in Fig. 1, panel A). Large complexes form, with a mean size of 300 nm; they appear globular in shape, with roundish edges, suggesting that different polyion-coated vesicles begin to aggregate, maintaining their individuality (Fig. 4, panel A). Within the clusters, globular regions, with the typical size of the original

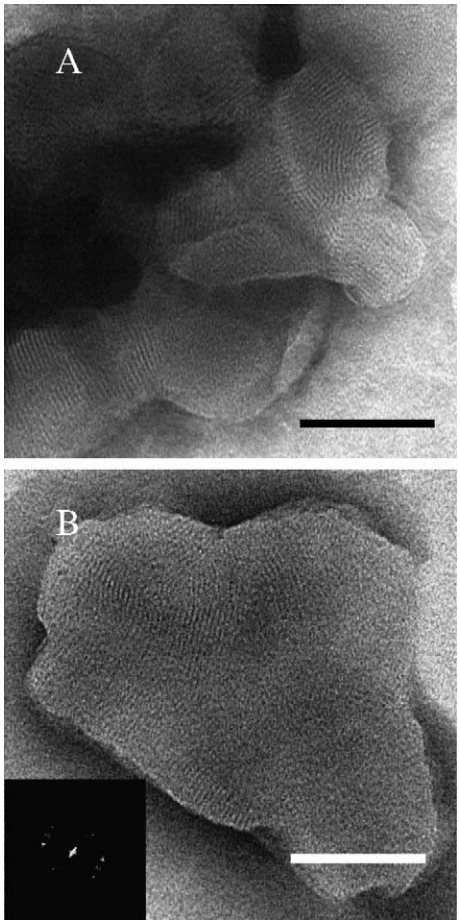

Fig. 4. TEM images (negative staining) of dsDNA–DOTAP complexes at N^-/N^+=0.25 (concentration marked by the letter b) in panel A of Fig. 1). Panel A: general view of a typical complex; the spherical polyion-coated liposomes are clearly recognizable; bars represent 100 nm. Panel B: a typical isolated dsDNA–DOTAP complex. In the inset in panel B, the FFT of the pattern on the complex is shown. The ordered disposition of DNA polyions, condensed on the liposome surface, shows an inter-helical distance of about 4 nm.

liposomes (100 nm), are clearly distinguishable, suggesting that clusters are composed of liposomes "glued together". These globular regions are covered by a characteristic "fingerprint" pattern probably due to the organization of the DNA molecules adsorbed at the liposome surface. The inset of panel B, Fig. 4 shows a two dimensional Fourier Transform of the image, from which a characteristic repetition length of ≈4 nm is obtained. Several different frames have been analyzed in this way, obtaining an average value of 4±1 nm.

When the polyion content is further increased, up to a polyion/lipid ratio $N^-/N^+=1$, the size of the clusters increases as well. However, the morphology they show is similar to that of Fig. 4, but with a larger number of the vesicles forming the clusters (images not shown).

In the presence of ssDNA polyion, at a charge ratio of $N^-/N^+=0.1$, complexes appear similar to those formed with dsDNA at low polyion content: isolated polyion-coated liposomes are observed. Fig. 5 shows a single-coated liposome and, in the inset, a magnification of polyion coating. The thickness measured for this ssDNA adsorbed layer is ~15 nm, larger than the one measured at a similar polyion content for the stiffer dsDNA chain. When charge ratio approaches $N^-/N^+=0.15$ and the hydrodynamic radius of the complex, as observed by DLS, increases, large aggregates form. As in the case of dsDNA, these aggregates appear formed by vesicles that maintain their individuality inside the cluster (Fig. 6, panel A). The size of these structures progressively increases up to a charge ratio of $N^-/N^+=0.2$, where a maximum is reached and, as in the case of dsDNA, with a further increase in polyion content, their size progressively decreases, until they are again replaced by polyion-coated isolated liposomes.

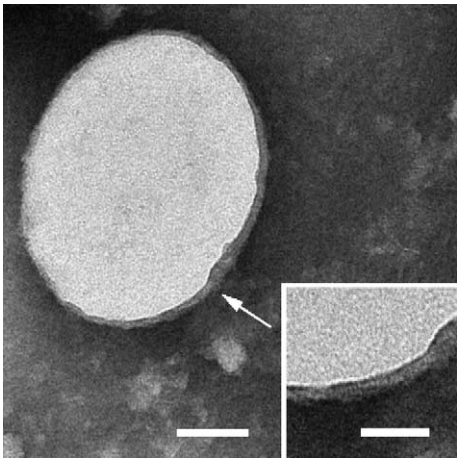

Fig. 5. TEM image (negative staining) of ssDNA–DOTAP complexes at $N^-/N^+=0.1$, (concentration marked by the letter (a) in panel B of Fig. 1). Spherical isolated polyion-coated liposomes form, with the adsorbed polyions that form a diffuse layer on the surface, well visible at the border of the vesicles; bar represents 100 nm. Inset shows the polyion coating; bar represents 50 nm.

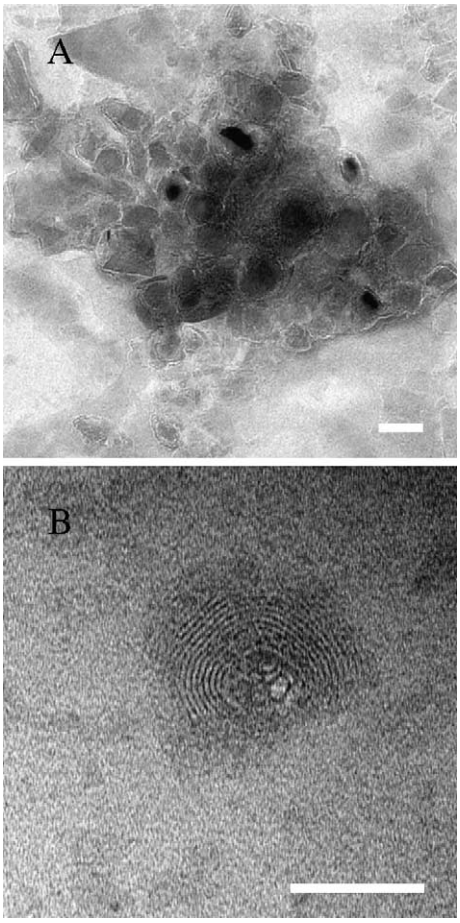

Fig. 6. Panel A: TEM image (negative staining) of ssDNA–DOTAP complexes at $N^-/N^+=0.15$, (concentration marked by the letter b) in panel B of Fig. 1). Polyion-coated liposomes form a large globular complex; bar represents 100 nm. Panel B: at $N^-/N^+=0.25$, at large polyion content, the ssDNA pattern on the surface of some complexes is observed (bar is 100 nm).

For the two DNA polyions, a remarkable difference exists in the surface coverage, since the ordered pattern characterizing the structures formed in the presence of dsDNA (Fig. 4) is observed for ssDNA only in a few frames and only on very small portions of the aggregate surface (Fig. 6, panel B). At very low polyion content, also the structures formed in the presence of NaPAA appear as isolated liposomes with adsorbed polyions, but now the adsorbed layer is even more thick than for ssDNA, extending, on average, to a length in the order of 30 nm for the polymer with a Mw 60 kDa, and with a 'wooly' appearance (images not shown). This appearance and the large thickness of the layer can be due to the fact that the polymer chains are in a (more or less deformed) random coil conformation. Above a charge ratio $N^-/N^+>0.5$, larger and larger structures appear (Fig. 7). They reach their maximum size at $N^-/N^+\approx 1$, and then decrease continuously in size beyond this point. However, in the whole concentration range, the morphology, as revealed by TEM for these aggregates, remains qualitatively the same and only the size

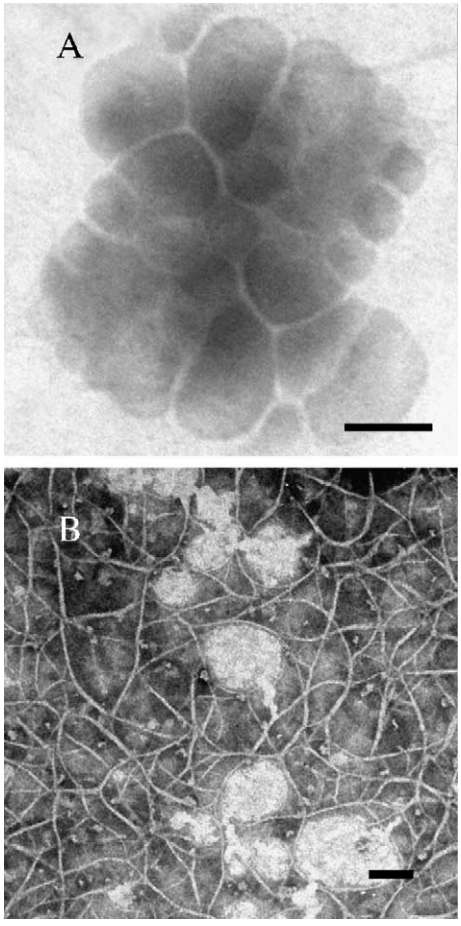

Fig. 7. TEM images of NaPAA–DOTAP complexes at charge ratio $N^-/N^+=0.65$, at moderate polyion concentration (concentration marked by the letter b) in the panel B of Fig. 2). Bars represent 100 nm. Panel A: the aggregates can be imaged without any staining by using TEM images in Electron Spectroscopy Imaging (ESI) mode. Liposomes within the aggregate maintain their approximately spherical shape. Panel B: the negative staining of the sample reveals the network of the polyion as elongated ribbons or threads which attack the clusters of vesicles; each individual thread has an apparent thickness of about 4 nm.

of the clusters changes. As an example, Fig. 7, panel A, shows an image of NaPAA–DOTAP complexes at $N^-/N^+=0.6$ obtained by using TEM in electron spectroscopy imaging (ESI) mode, without any staining. Liposomes apparently stick to each other without fusing, maintaining their spherical shape and individuality. Negative staining (Fig. 7, panel B) evidences new details in the clusters: outlines of the liposome are now barely visible while a network of elongated ribbons and threads interweaves the vesicles. An analysis at a higher magnification (images not shown) of the dimensions of the individual threads of this network reveals an apparent thickness of about 4 nm; this value should only be considered as an indication since the resolution limit of the technique is of about 2 nm.

In order to clearly attribute the observed striations in Figs. 4 and 6 as due to DNA polyion coating the cationic liposomes, we have performed an independent measurement of DNA-induced liposome aggregates using biotinylated DNA and revealing the adsorbed DNA by using gold-labeled streptavidin.

In Fig. 8, a typical TEM image (negative staining) of biotinylated DNA–DOTAP complexes at $N^-/N^+=0.48$ is shown. The whole surface of the liposome aggregate, where individual vesicles are clearly proved by the different degree of staining, is sprinkled with gold particles (10 nm in diameter), evidencing that on the aggregate surface biotinylated DNA is available for complexation by gold-conjugated streptavidin. This result strongly strengthens that DNA, in the structures we are considering, is adsorbed on the liposome surface, rather than "sandwiched" between lipid bilayers or entrapped within the "pipes" of a hexagonal lipid phase. Moreover, although the expected number of gold particles per unit aggregate surface is difficult to be evaluated, depending on the biotinylated sites available for streptavidin, we have found, in all the samples investigated, that the gold particle concentration in biotinylated DNA–liposome aggregates is two order of magnitude larger than the concentration found in non-biotinylated DNA–liposome aggregates treated with gold-labeled streptavidin. In this latter case, only a few particles remain entrapped at the aggregate surface, showing no preference for liposome aggregates or for the bare carbon film surface. Panels B and C in Fig. 8 show, at a higher magnification (4.2×), an ordered pattern similar to those observed in Figs. 4 and 6, where gold particles lie over the pattern, demonstrating that the pattern itself can be due to almost partially ordered DNA chains.

In order to further investigate the role of electrostatic interactions on the complexation mechanism, we have varied the ionic strength of the aqueous phase, (i.e., the Debye screening length for electrostatic interactions), by adding a simple electrolyte, NaCl, at different final concentrations in the range from 0.005 M to 0.5 M. Consequently, the Debye screening length varies from about 4 nm to about 0.4 nm. The size of the complexes resulting from DOTAP liposomes and NaPAA polyions (molecular weight 60 kDa) at varying the electrolyte concentrations is shown in Fig. 9, for three different polyion–lipid (N^-/N^+) charge ratios. As can be seen, for the same adsorbed polyion content, the size of the aggregates increases with the salt content. However, for all the concentrations shown, the aggregates appear stable in time, and only at much higher ionic strength destabilization occurs and the suspension eventually flocculates rapidly.

Finally, we have checked the *equilibrium* character of the aggregates by mixing two different samples of DOTAP-NaPAA 60 kDa with the same polyion content (corresponding to $N^-/N^+=0.5$), but prepared at two different NaCl electrolyte concentrations, 0.004 mol/l for sample A and 0.35 mol/l for sample B, respectively. The corresponding particle size distributions are shown in Fig. 10, panels A (top) and B (bottom). In panel C (center), we report (empty bars) the size distribution of a 1:1 vol/vol mixture of samples A and B, the resulting NaCl concentration being 0.17 mol/l. This distribution is compared with the size

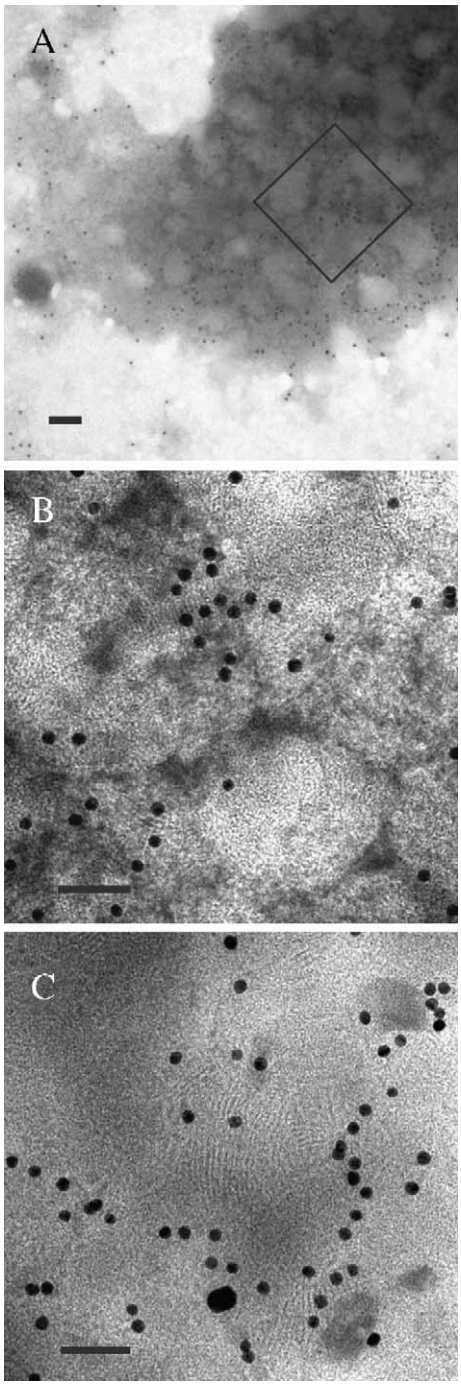

Fig. 8. Panel A: TEM image (negative staining) of biotinylated DNA–DOTAP complexes at $N^-/N^+=0.48$. Within large aggregates, the contours of the individual vesicles are clearly discernible. The whole surface of liposome aggregates is covered by gold particles (10 nm diameter); bar represents 100 nm. Panel B: at a higher magnification, an ordered pattern observed for both dsDNA and (rarely) for ssDNA on the surface of complexes is observed and, in some cases, the gold particles seems to crowd around and over the ordered zones. (B) is a 4.2× magnification of the area enclosed in the box in panel A. Bar is 50 nm. Panel C: a further example of DNA striation at the liposome surface marked by gold particles. Bar is 50 nm.

distribution (full bars) of a sample which was directly prepared at the final NaCl concentration of 0.17 mol/l. The almost perfect coincidence of these two distributions gives

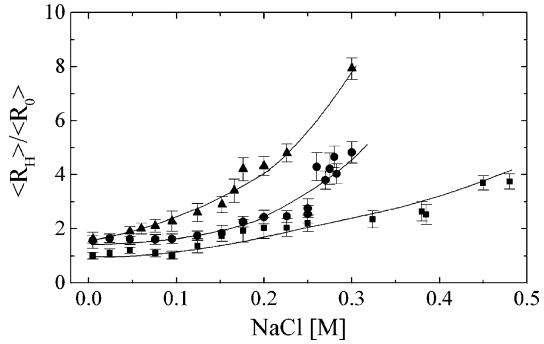

Fig. 9. Average equilibrium radius $<R_H>$ of DOTAP–NaPAA 60 kD complexes, normalized respect to liposome radius $<R_O>$, at increasing NaCl concentration, for three different polyelectrolyte/lipid charge ratios: ▲, $N^-/N^+=0.64$; ●, $N^-/N^+=0.53$; ■, $N^-/N^+=0.26$. Full lines serve to guide the eyes, only.

evidence of the reversible character of the lipoplex aggregation, qualifying the clusters as 'true equilibrium' aggregates, as opposed to 'kinetically stabilized' aggregates. It must be noted that to obtain the size distributions shown in Fig. 10, the DLS autocorrelation functions have been carefully analyzed by using both NNLS and CONTIN analyses to eliminate possible sources of error due to the choice of the procedure. We report here the NNLS size distribution, the two resulting size distributions being equivalent. By using as a test sample a 1:1 vol/vol mixture of two different standard polystyrene latex suspensions with sizes comparable with the lipoplexes in sample A and in sample B, respectively, we have also checked that, in similar experimental conditions, the two population are well distinguished as separate populations (data not shown).

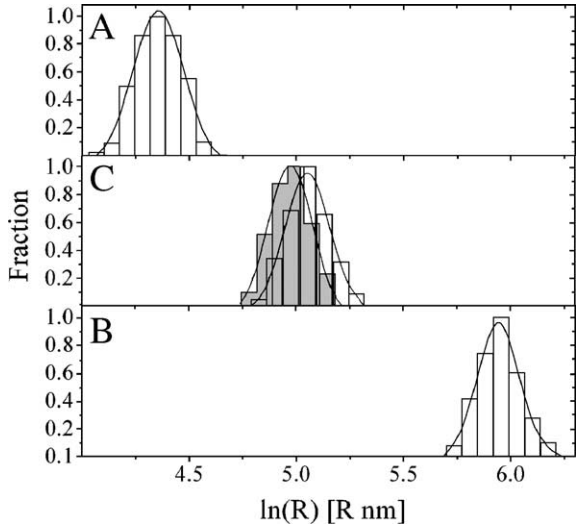

Fig. 10. Intensity weighed particle size distribution of DOTAP–NaPAA complexes at fixed polyelectrolyte/lipid charge ratio ($N^-/N^+=0.5$) and different NaCl electrolyte concentration. Upper panel A: sample 0.004 mol/l, bottom panel B: sample 0.35 mol/l, center panel C: sample obtained by mixing A and B in equal volume (empty bars) in comparison to the sample obtained by adding NaCl to the complex suspension to a final concentration of 0.17 mol/l (full bars).

4. Discussion

The phenomenology of the complexation process observed in this work is qualitatively the same for the three polyions employed, showing a definite trend of the hydrodynamic radius as a function of the polyion concentration (Figs. 1 and 2). As it has been already reported by other authors [56], at increasing charge ratio, lipoplexes condense in large aggregates whose size increases smoothly, reaches its maximum at the isoelectric point and then decreases again, showing the typical behavior that is usually termed "reentrant" condensation. Although this qualitative behavior was observed for all the three polyions employed (dsDNA, ssDNA and NaPAA), the charge ratio value for ssDNA, where this maximum is attained, is apparently different from the other two polyions. Moreover, for the NaPAA polyion, a marked difference in the maximum size reached by the aggregates is observed for the three different molecular weights employed (the longer the polymer, the larger the aggregates).

For the three polyions dsDNA, ssDNA and NaPAA investigated, TEM measurements on their complexes with DOTAP liposomes show that complexes occur without the rupture of the vesicles and a complete destabilization of the lipid double layers and large clusters form as the result of polyion-coated liposomes aggregation. The globular appearance of the objects forming the clusters that have the typical dimensions of an original liposome (≈100 nm in diameter) is well identified in the images shown in Figs. 4, 6 and, in the case of Fig. 7 panel A, vesicles as individual structures clearly appear. These findings partially conflict with the picture of lipoplexes considered as well-ordered multilayers or hexagonal aggregates [14,56]. However, similar structures formed by aggregation of undestroyed vesicles have been already observed by Cryo-TEM electron microscopy in the complexes between the DNA and cationic DMPC/DC-Chol liposomes, close to the charge neutralization [60]. In the images reported by these authors, besides multilamellar structures, aggregates of intact DNA decorated liposomes are clearly visible.

While the underlying aggregation mechanism is similar for ssDNA and ds-DNA, remarkable differences are observed in the surface coverage realized by these two polyions. A liquid crystal pattern is observed in all the images showing dsDNA samples (Fig. 4). On the contrary, there is no evidence that ss-DNA forms an ordered pattern on vesicle surface, both in the case of isolated vesicles (Fig. 5) and of large aggregates (Fig. 6 panel A). Only at the highest ssDNA concentrations, corresponding to charge ratios $\geq N^-/N^+ = 0.25$, ordered DNA patterns are occasionally observed (panel B of Fig. 6). The ordered pattern observed on the surface of the globular structures should be attributed to the organization of DNA molecules onto liposome surface, as it has been observed in supported cationic lipid membranes investigated by means of high resolution AFM measurements [61–63]. Images reported in Fig. 4 clearly show DNA polyions realizing a two-dimensional ordered structure, where the chains arrange in a correlated organization in parallel arrays with fixed inter-helical distance similar to the one observed in AFM measurements. In Fig. 4, the bends where the chains modify the adsorption direction can be clearly individuated. By means of a two dimensional Fourier Transform (FFT) analysis (Fig. 4, panel B), a constant inter-helical distance of about 4 ± 1 nm is obtained for all the complexes analyzed. This value is in good agreement with the average inter-helical distance of condensed DNA on cationic DPTAP bilayers measured on AFM images (about 5 nm for DNA helices adsorbed on DPTAP bilayer [61], values between 4.3 and 5.8 nm [62] for different bulk NaCl concentration and an average spacing of 6.5 ± 0.4 for DNA adsorbed to a supported DPTAP bilayers [63]). In our TEM images, due to the reduced lateral resolution of this technique, ordered patterns on the surface of ssDNA lipoplexes are seldom observed, and the adsorbed polyion layer at the surface of these lipoplexes shows a 'wooly' appearance (Fig. 5) and a larger thickness compared to the smooth layer adsorbed on dsDNA lipoplexes (Fig. 3).

This overall phenomenology is associated to the correlated adsorption of polyions as predicted by the theory of macroion charged surface interactions [17]. It has been shown that correlated adsorption of polyions on oppositely charged macroions (cationic liposomes, in our case) gives rise to the phenomenon of overcharging or charge inversion [17,23,24]. As it has been pointed out by, among others, Grønbech-Jensen et al. [25] and Shklovskii et al. [26], long range order of the adsorbed polyions is not essential for inducing charge inversion, only *correlation* and *short range* order are needed. "Correlated" adsorption is another way to indicate a non-random and essentially non-homogeneous charge distribution at the polyion decorated liposome surface. Adsorbed polyions, avoiding each other and residing as far away as it is possible to minimize their electrostatic interactions, form at the lipoplex surface a (short-range) ordered pattern that is the origin of an attractive potential ("charge patch" attraction) [27,28,64]. When almost-neutral complexes approach, a local 'dipolar' attraction between the polyion-coated domains on one complex (excess of negative charge) and the polymer-free domains on another complex (excess of positive charge) promotes their binding. Assuming the short-range attractive potential independent of the size of the aggregate and only dependent on the local surface characteristics, close to the isoelectric point, large aggregates can form; the smaller the strength of the electrostatic repulsion, the larger the number of DNA-decorated liposomes which can stick together. Such a mechanism is able to explain both the observed *continuous* dependence of the *size* of the aggregates on the polyion/lipid N^-/N^+ ratio (Figs. 1 and 2) and the equilibrium character of these aggregates, as evidenced by the reversibility of the aggregative process (Fig. 10). Moreover, the dependence of the size of the aggregates

on the ionic strength of the suspension (Fig. 9) gives evidence for the electrostatic nature of the interactions governing this equilibrium.

The strength of the attractive potential depends on the polyion coverage since a uniform coverage results in less surface charge inhomogeneity and, consequently, in weaker attraction, the more uniform charge distribution being realized by shorter polyions. This mechanism justifies the dependence of the cluster size on the polyion length. As clearly visible in the presence of NaPAA polyelectrolyte (Fig. 2), larger clusters are formed by longer polyions, i.e., with higher molecular weights. The average radius of these aggregates spans from 300 to 650 nm, with increasing of the molecular weight from 5.1 to 225 kDa. Due to the comparatively short length of the polyions employed, with respect to the typical liposome radius (polyion contour length ranges from ≈10 nm for Mw 5.1 kDa to ≈450 nm for 225 kDa), 'bridging' effects do not play a significant role in aggregation. A similar dependence on the degree of polymerization has been observed for ssDNA-induced flocculation of polystyrene colloidal particles [64].

Recently, Groenewold and Kegel [65] showed that a small charge is sufficient to stabilize clusters with large aggregation number in colloidal suspensions characterized by attractive interactions between particles. By minimizing the free energy per particle in a cluster, these authors [65] found that the equilibrium aggregation number n_0 is given by

$$n_0 = \frac{8\pi\epsilon_0\epsilon\gamma v_0}{(z_0 e)^2} \tag{4}$$

where γ is the negative excess energy per unit surface associated to the particle at the cluster surface, v_0 the volume of the "elementary" aggregating particle that contributes to the cluster formation and $z_0 e$ the charge per particle. Assuming for $\gamma = 0.3$ mJ/m^2 (of the same order of magnitude of interactions between phosphatidylcholine bilayers [66]), with the permittivity of the aqueous phase $\epsilon = 80$, the volume of a single polyion-coated particle $v_0 = 2.5\ 10^{-16}$ cm^3, the charge $z_0 e = 10$ elementary charges, we obtain an aggregation number n_0 of the order of 5×10^2, which yields a cluster of size of the order of $R_H = 350–400$ nm, in good agreement with the value derived from light scattering measurements (the maximum observed in Fig. 2 at $N^-/N^+ \simeq 1$).

If the formation of aggregates is interpreted according to the "overcharging" and "charge patch" attraction mechanism, since the vesicles remain substantially undestroyed in the complexation, the maximum of the aggregation has to be observed when the adsorbed polyions nearly exactly counterbalance the external surface charge of the liposomes. It is noteworthy that, recently, Ciani et al. [67] reached the same conclusion on the basis of their investigation of DOTAP/DOPE and DC-Chol/DOPE lipoplexes by means of zeta potential and electron spin resonance measurements. According to Eq. (3), the isoelectric point should then correspond to a charge ratio of $N^-/N^+ = 0.5$, since only the external surface charge on the liposomes is involved, assuming, to this level of approximation, the same radius for the outer and inner leaflet of the vesicle bilayer. However, in the presence of dsDNA and NaPAA polyions, the localization of the peak occurs at $N^-/N^+ \sim 1$, while, in the case of the ss-DNA, we found the peak at $N^-/N^+ \sim 0.2$. This apparent inconsistency can be overcome if a proper charge re-normalization is introduced, both for the polyion charge [29] and for the liposome charge [68,69].

More extensively, according to Manning [29], the relevant structural parameter for a linear charged polyion is the charge density parameter $\xi = l_B/b$, where l_B is the Bjerrum length ($l_B = e^2/(4\pi\epsilon_0\epsilon_w k_B T)$ characterizes the intensity of electrostatic interactions; in water at $T = 25$ °C, $l_B \approx 7.14$ Å) and b is the average spacing between adjacent charges on the chain axis. At infinite dilution, Manning's theory predicts a fraction of condensed counterions equal to $1 - 1/(z\xi)$, where z is the counterion valence. For dsDNA, $b = 1.7$ Å and the fraction of neutralized charges is equal to 76% in the presence of monovalent counterions. For ssDNA chains, b is in the order of 10 Å [70] and the counterion condensation ($\xi < 1$) is negligible. For NaPAA, with $b = 1.8$ Å and $\xi \approx 4$, the extent of condensation is approximately the same as for dsDNA.

By taking into account the counterion condensation, the neutralization condition should then be written as $2\ fN^-/gN^+ = 1$, where f and g represent the fractions of "effective" ionized groups on the polyion and liposome, respectively, and the factor 2 simply comes from considering only the charges on the liposome external surface. The assumption that the fraction of counterions condensed on a polyion close to an oppositely charged surface is given by the Manning expression is an oversimplification. However, it has been shown that, also for rigid rod-like polyions as dsDNA, counterions can remain partly condensed when the polyion is close to a charged surface [20]. By calculating the condensed fraction of counterions using the Manning theory, both for dsDNA polyion and NaPAA polyion (that approximately have the same charge for unit length), the fraction of condensed counterions should be 0.76, while for ssDNA, the counterion condensation is negligible, owing to its low charge density ($\xi < 1$). In the case of ssDNA, since no condensation occurs ($f = 1$), it is possible to evaluate the fraction g of charge on the liposome. Considering that the maximum size is in this case at $N^-/N^+ = 0.2$, the neutralization condition yields the value $g = 0.4$. Using this value for the other two polyions investigated, we estimated $f \simeq 0.20$ for dsDNA ($N^-/N^+ \simeq 1$) and $f \simeq 0.18$ for NaPAA ($N^-/N^+ \simeq 1.1$). These values of f are in qualitative agreement with the ones that could be calculated according to the Manning theory, $f \sim 0.24$ for both dsDNA and NaPAA polyions.

These results are in agreement with the results of Ciani et al. [67] on synthetic oligonucleotides. By means of zeta potential measurements, for DC-Chol/DOPE–DNA lipoplexes, they determine the isoelectric point at a value $N^-/N^+ = 0.4 \div 0.6$ for dsDNA and at a lower charge ratio, at $N^-/N^+ = 0.2 \div 0.3$, for ssDNA.

Further evidence for a comprehensive picture is obtained from the surface organization of polyions, as deduced from Fig. 5, where the thickness of the polyion adsorbed layer can be evaluated. Dobrynin et al. [18,19], on the basis of a scaling analysis, have described different polyion adsorption regimes, depending on the surface charge density. For a flexible polyion chain, the key parameters that govern the adsorption process and the resulting structural organization are the monomer size b, the degree of polymerization N, the fraction f of free counterions and the Bjerrum length l_B. In the case of a polyion with structural and charge properties of the ssDNA ($b=1$ nm, $N=700$, $f=1$) and a surface charge density corresponding to a full ionization, an adsorption thickness of the order of 1 nm, comparable to the lateral dimension of the chain, is expected. On the contrary, the observed value is the order of 15 nm, a value that within the model would be compatible only with a much lower surface charge density, giving support to the hypothesis of a strong neutralized charge. In the case of dsDNA, a similar estimate of the adsorbed layer thickness (Fig. 3) gives a value of the order of 7 nm, again in qualitative agreement with the Dobrynin et al. model [18,19], considering the higher structural charge density of this polymer.

A final comment on the extent of counterion condensation is in order. Complete or partial release of condensed counterions has been invoked as the 'driving force' for polyion adsorption at liposome surface, and different theories show that counterions can be "completely" released [71], "mostly released" [72], "partially" released [21], "not always released" [20] or not released at all (in the case of flexible polyelectrolytes) [19]. The phase behavior of cationic lipid–DNA complexes has been analyzed on this basis [31,32]. However, our results give further support to the aggregation governed by correlation, the extent of counterion release appearing a secondary factor in driving polyelectrolyte adsorption.

In conclusion, the results presented here and the overall description adopted here seem to be in reasonable agreement with a polyion–liposome complexation scenario where the adsorbed polyion correlation represents the "driving force" for the formation of large equilibrium aggregates, giving rise to a "reentrant" condensation with the increase of the polyion–liposome charge ratio, through the balance of "charge patch" attraction, due to the correlated adsorption of polyions at the liposome surface, and the weak repulsion close the isoelectric point.

References

[1] D. Ferber, Gene therapy: safer and virus-free? Science 294 (2001) 1638–1642.

[2] M. Pedroso De Lima, S. Simoes, P. Pires, H. Faneca, N. Duzgunes, Cationic lipid–DNA complexes in gene delivery: from biophysics to bio-physical applications, Adv. Drug Deliv. Rev. 47 (2001) 277–294.

[3] M.C. Woodle, P. Scaria, Cationic liposomes and nucleic acids, Curr. Opin. Colloid Interface Sci. 6 (2001) 77–86.

[4] M. Nishikawa, L. Huang, Nonviral vectors in the new millennium: delivery barriers in gene transfer, Hum. Gene Ther. 12 (2001) 861–870.

[5] D. Lasic, Liposomes in Gene Delivery, RCR Press, Boca Raton, FL, 1997.

[6] S. Hui, M. Langner, Y. Zhao, P. Ross, E. Hurley, K. Chan, The role of helper lipids in cationic liposome-mediated gene transfer, Biophys. J. 71 (1996) 590–599.

[7] C.J. Wheeler, P.L. Felgner, Y.J. Tsai, J. Marshall, S.G. Sukhu, L. Doh, J. Hartikka, J. Nietupski, M. Manthorpe, M. Nichols, M. Plewe, X. Liang, J. Norman, A. Smith, S.H. Cheng, A novel cationic lipid greatly enhances plasmid DNA delivery and expression in mouse lung, Proc. Natl. Acad. Sci. U. S. A. 93 (1996) 11454–11459.

[8] A. Martin-Herranz, A. Ahmad, H.M. Evans, K. Ewert, U. Schulze, C.R. Safinya, Surface functionalized cationic lipid–DNA complexes for gene delivery: PEGylated lamellar complexes exhibit distinct DNA–DNA interaction regimes, Biophys. J. 86 (2004) 1160–1168.

[9] N.J. Zuidam, D. Hirsch-Lerner, S. Margulies, Y. Barenholz, Lamellarity of cationic liposomes and mode of preparation of lipoplexes affect transfection efficiency, Biochim. Biophys. Acta 1419 (1999) 207–220.

[10] J. Smisterova, A. Wagenaar, M.C.A. Stuart, E. Polushkin, G. Ten Brinke, R. Hulst, J.B. Engberts, D. Hoekstra, Molecular shape of the cationic lipid controls the structure of cationic lipid/dioleylphosphatidylethanolamine–DNA complexes and the efficiency of gene delivery, J. Biol. Chem. 276 (2001) 47615–47622.

[11] A.J. Lin, N.L. Slack, A. Ahmad, C. George, C.E. Samuel, C.R. Safinya, Three-dimensional imaging of lipid gene-carriers: membrane charge density controls universal transfection behaviour in lamellar cationic–DNA complexes, Biophysical J. 84 (2003) 3307–3316.

[12] B. Stenberg, F. Sorgi, L. Huang, New structures in complex formation between DNA and cationic liposomes visualized by freeze fracture electron microscopy, FEBS Lett. 356 (1994) 361–366.

[13] D.D. Lasic, H. Strey, M.C.A. Stuart, R. Podgornik, P.M. Fredick, The structure of DNA–liposome complexes, J. Am. Chem. Soc. 119 (1997) 832–833.

[14] J.O. Rädler, I. Koltover, T. Salditt, C.R. Safinya, Structure of DNA-cationic liposome complexes: DNA intercalation in multilamellar membranes in distinct interhelical packing regimes, Science 275 (1997) 810–814.

[15] I. Koltover, T. Salditt, J.O. Rädler, C.R. Safinya, An inverted hexagonal phase of cationic liposome–DNA complexes related to DNA release and delivery, Science 281 (1998) 78–81.

[16] D. Simberg, D. Danino, Y. Talmon, A. Minsky, M.E. Ferrari, C.J. Wheeler, Y. Barenholz, Phase behavior, DNA ordering, and size instability of cationic lipoplexes, J. Biol. Chem. 276 (2001) 47453–47459.

[17] A.Y. Grosberg, T.T. Nguyen, B.I. Shklovskii, Colloquium: the physics of charge inversion in chemical and biological systems, Rev. Mod. Phys. 74 (2002) 329–345.

[18] A.V. Dobrynin, A. Deshkovski, M. Rubinstein, Adsorption of polyelectrolytes at oppositely charged surface, Macromolecules 34 (2001) 3421–3436.

[19] A.V. Dobrynin, A. Deshkovski, M. Rubinstein, Adsorption of polyelectrolytes at oppositely charged surface, Phys. Rev. Lett. 84 (2000) 3101–3104.

[20] P. Sens, J.F. Joanny, Counterion release and electrostatic adsorption, Phys. Rev. Lett. 84 (2000) 4862–4865.

[21] T.T. Nguyen, A.Y. Grosberg, B.I. Shklovskii, Macroions in salty water with multivalent ions: giant inversion of charge, Phys. Rev. Lett. 85 (2000) 1568–1571.

[22] T.T. Nguyen, B.I. Shklovskii, Complexation of DNA with positive

spheres: phase diagram of charge inversion and reentrant condensation, J. Chem. Phys. 115 (2001) 7298–7308.
[23] T.T. Nguyen, B.I. Shklovskii, Overcharging of macroion by an oppositely charged polyelectrolyte, Physica A 293 (2001) 324–338.
[24] E. Mateescu, C. Jeppepsen, R. Pincus, Overcharging of a spherical macroion by an oppositely charged polyelectrolyte, Europhys. Lett. 46 (1999) 493–498.
[25] N. Grønbech-Jensen, R.J. Mashl, R.F. Bruinsma, W.M. Gelbart, Counterion-induced attraction between rigid polyelectrolytes, Phys. Rev. Lett. 78 (1997) 2477–2480.
[26] T.T. Nguyen, B.I. Shklovskii, Wigner crystal model of counterion induced bundle formation of rodlike polyelectrolytes, Phys. Rev. Lett. 82 (1999) 3268–3271.
[27] S.J. Miklavic, D.Y.C. Chan, L.R. White, T.W. Healy, Double layer forces between heterogeneous charged surfaces, J. Phys. Chem. 98 (1994) 9022–9032.
[28] A.V.M. Khachatourian, A.O. Wistrom, Electrostatic interaction force between planar surfaces due to 3-d distribution of sources of potential (charge), J. Phys. Chem., B 102 (1998) 2483–2493.
[29] G.S. Manning, The molecular theory of polyelectrolyte solutions with applications to the electrostatic properties of polynucleotides, Q. Rev. Biophys. 11 (1978) 179–246.
[30] R. Bruinsma, Electrostatics of DNA–cationic lipid complexes: isoelectric instability, Eur. Phys. J., B 4 (1998) 75–88.
[31] D. Harries, S. May, W.M. Gelbart, A. Ben-Shaul, Structure, stability, and thermodynamics of lamellar DNA–Lipid complexes, Biophys J. 75 (1998) 159–173.
[32] S. May, D. Harries, A. Ben-Shaul, The phase behavior of cationic lipid DNA complexes, Biophys. J. 78 (2000) 1681–1697.
[33] F. Bordi, C. Cametti, M. Diociaiuti, D. Gaudino, T. Gili, S. Sennato, Complexation of anionic polyelectrolytes with cationic liposomes: evidence of reentrant condensation and lipoplex formation, Langmuir 20 (2004) 5214–5222.
[34] S. Sennato, F. Bordi, C. Cametti, On the phase diagram of reentrant condensation in polyelectrolyte–liposome complexation, J. Chem. Phys. 121 (2004) 4936–4940.
[35] S. Sennato, F. Bordi, C. Cametti, Correlated adsorption of polyelectrolytes in the charge inversion of colloidal particles, Europhys. Lett. 68 (2004) 296–302.
[36] F. Bordi, C. Cametti, T. Gili, D. Gaudino, S. Sennato, Time evolution of the formation of different size cationic liposome–polyelectrolyte complexes, Bioelectrochemistry 59 (2003) 99–106.
[37] V. Kumaran, Instabilities due to charge-density-curvature coupling in charged membranes, Phys. Rev. Lett. 85 (2000) 4996–4999.
[38] V. Kumaran, Effect of surface charge on the curvatura moduli of a membrane, Phys. Rev., E 64 (2001) 051922/1–051922/9.
[39] D.E. Kohne, S.A. Levison, M.J. Byers, Room temperature method for increasing the rate of DNA reassociation by many thousandfold: the phenol emulsion reassociation technique, Biochemistry 16 (1977) 5329–5341.
[40] N.M. Green, Avidin, Adv. Protein Chem. 29 (1975) 85–133.
[41] J. Sambrook, E.F. Fritsch, T. Maniatis, Molecular Cloning: A Laboratory Manual, Cold Spring Harbor Laboratory Press, Cold Spring Harbor, NY, 1989.
[42] C. Blasi, P. Pilo Boyl, M. Ledda, A. Novolletto, K. Gibson, C. Jakobs, B. Hogema, S. Akaboshi, F. Loreni, P. Malaspina, Structure of human succinic semialdehyde dehydrogenase gene: identification of promoter region and alternatively processed isoforms, Mol. Genet. Metab. 76 (2002) 348–362.
[43] B.J. Berne, R. Pecora, Dynamic Light Scattering, Wiley, New York, 1976.
[44] P. Štěpánek, Data analysis in dynamic light scattering, in: W. Brown (Ed.), Dynamic Light Scattering: the Method and Some Applications, Clarendon Press, Oxford, 1993, pp. 177–241.
[45] L.H. Hanus, H.J. Ploehn, Conversion of intensity-averaged photon correlation spectroscopy measurements to number-averaged particle size distribution, Langmuir 15 (1999) 3091–3100.
[46] H. Ruf, B.J. Gould, H.W., The effect of nonrandom errors on the results from regularized inversions of dynamic light scattering data, Langmuir 16 (2000) 471–480.
[47] I.D. Morrison, E.F. Grabowski, Improved techniques for particle size determination by quasi-elastic light scattering, Langmuir 1 (1985) 496–501.
[48] S. Provencher, A constrained regularization method for inverting data represented by linear algebraic or integral equations, Comput. Phys. Commun. 27 (1982) 213–227.
[49] S. Provencher, CONTIN: a general purpose constrained regularization program for invering noisy linear algebraic and integral equations, Comput. Phys. Commun. 27 (1982) 229–242.
[50] C.L. Lawson, I.D. Morrison, Solving Least Squares Problems. A FOR-TRAN Program and Subroutines Called NNLS, Prentice-Hall, Englewood Cliffs, NJ, 1974.
[51] J. Gustafssonn, G. Arvidson, G. Karlsson, M. Almgrem, Complexes between cationic liposomes and DNA visualized by cryo-TEM, Biochim. Biophys. Acta 1235 (1995) 305–312.
[52] I. Pasquali-Ronchetti, D. Quaglino, G. Mori, B. Bacchelli, Hyaluronan–phospholipid interactions, J. Struct. Biol. 120 (1997) 1–10.
[53] E. Lai, J.H. van Zanten, Real time monitoring of lipoplex molar mass, size and density, J. Control. Release 82 (2002) 149–158.
[54] E. Lai, J.H. van Zanten, Evidence of lipoplex dissociation in liquid formulation, J. Pharmacol. Sci. 91 (2002) 1225–1232.
[55] P. Pires, S. Simoes, S. Nir, R. Gaspar, N. Duzgunes, M. Pedroso de Lima, Interactions of cationic liposomes and their DNA complexes with monocytes leukemia cells, Biochim. Biophys. Acta 1418 (1999) 71–84.
[56] J.O. Rädler, I. Koltover, A. Jamieson, T. Salditt, C.R. Safinya, Structure and interfacial aspects of self-assembled cationic lipid–DNA gene carrier complexes, Langmuir 14 (1998) 4272–4283.
[57] W.B. Russel, D.A. Saville, W.R. Schowalter, Colloidal Dispersions, Cambridge Univ. Press, Cambridge, 1989.
[58] F. Bordi, R. Colby, C. Cametti, L. De Lorenzo, T. Gili, Electrical conductivity of polyelectrolyte solutions in the semidilute and concentrated regime: the role of counterion condensation, J. Phys. Chem., B 106 (2002) 6887–6893.
[59] A. De la Maza, L. Coderch, O. Lopez, J. Parra, Transmission electron microscopy and light scattering studies on the interaction of non-ionic/anionic surfactant mixtures with phosphatidylcholine liposomes, Microsc. Res. Tech. 40 (1998) 63–71.
[60] S. Huebner, B.J. Battersby, G. Grimm, G. Cevc, Lipid–DNA complex formation: reorganization and rupture of lipid vesicles in the presence of DNA as observed by cryoelectron microscopy, Biophys. J. 76 (1999) 3158–3166.
[61] J. Mou, D.M. Czajkowsky, Y. Zhang, Z. Shao, High-resolution atomic-force microscopy of DNA: the pitch of the double helix, FEBS Lett. 371 (1995) 279–282.
[62] Y. Fang, J. Yang, Two-dimensional condensation of DNA molecules on cationic lipid membranes, J. Phys. Chem., B 101 (1997) 441–449.
[63] H. Clausen-Schaumann, H.E. Gaub, DNA adsorption to laterally structured charged lipid membranes, Langmuir 15 (1999) 8246–8251.
[64] W.H. Walker, S.B. Grant, Factors influencing the flocculation of colloidal particles by a model anionic polyelectrolyte, Colloids Surf., A 119 (1996) 229–239.
[65] J. Groenewold, W.K. Kegel, Anomalous large equilibrium clusters of colloids, J. Phys. Chem., B 105 (2001) 11702–11709.
[66] R. Parthasarathy, J. Groves, Protein patterns at lipid bilayer junctions, Proc. Nat. Acad. Sci. 101 (2004) 12798–12803.
[67] L. Ciani, S. Ristori, A. Salvati, L. Calamai, G. Martini, DOTAP/DOPE and dc-chol/DOPE lipoplexes for gene delivery: zeta potential measurements and electron spin resonance spectra, Biochim. Biophys. Acta 1664 (2004) 70–79.
[68] W.L. Hsin, T.-Y. Wang, Y.-J. Sheng, H.-K. Tsao, Charge renormaliza-

tion of charged spheres based on thermodynamic properties, J. Chem. Phys. 121 (2004) 5494–5504.
[69] C. Haro-Pérez, M. Quesada-Pérez, J. Callejas-Fernández, E. Casals, J. Estelrich, R. Hidalgo-Álvarez, Liquidlike structures in dilute suspensions of charged liposomes, J. Chem. Phys. 118 (2003) 5167–5173.
[70] S. Neidle (Ed.), Oxford Handbook of Nucleic Acid Structure, Oxford Science Publication, 1999.
[71] C. Fleck, H.H. von Grünberg, Counterion evaporation, Phys. Rev., E 63 (2001) 061804/1–061804/5.
[72] S.Y. Park, R.F. Bruinsma, W.M. Gelbart, Spontaneous overcharging of macro-ion complexes, Europhys. Lett. 46 (1999) 454–460.